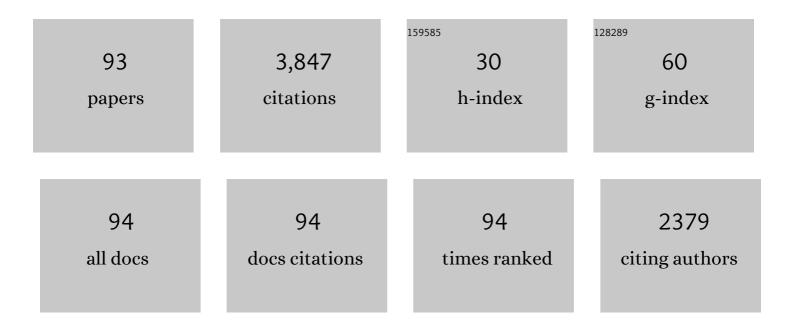
## **Robby Peibst**

List of Publications by Year in descending order

Source: https://exaly.com/author-pdf/1806377/publications.pdf Version: 2024-02-01



PORRY PEIRCE

#	Article	IF	CITATIONS
1	Laser contact openings for local poly-Si-metal contacts enabling 26.1%-efficient POLO-IBC solar cells. Solar Energy Materials and Solar Cells, 2018, 186, 184-193.	6.2	475
2	Surface passivation of crystalline silicon solar cells: Present and future. Solar Energy Materials and Solar Cells, 2018, 187, 39-54.	6.2	285
3	The 2020 photovoltaic technologies roadmap. Journal Physics D: Applied Physics, 2020, 53, 493001.	2.8	274
4	Recombination behavior and contact resistance of n+ and p+ poly-crystalline Si/mono-crystalline Si junctions. Solar Energy Materials and Solar Cells, 2014, 131, 85-91.	6.2	195
5	Working principle of carrier selective poly-Si/c-Si junctions: Is tunnelling the whole story?. Solar Energy Materials and Solar Cells, 2016, 158, 60-67.	6.2	177
6	Contact Selectivity and Efficiency in Crystalline Silicon Photovoltaics. IEEE Journal of Photovoltaics, 2016, 6, 1413-1420.	2.5	140
7	Ion Implantation for Poly-Si Passivated Back-Junction Back-Contacted Solar Cells. IEEE Journal of Photovoltaics, 2015, 5, 507-514.	2.5	131
8	2D/3D Heterostructure for Semitransparent Perovskite Solar Cells with Engineered Bandgap Enables Efficiencies Exceeding 25% in Fourâ€ferminal Tandems with Silicon and CIGS. Advanced Functional Materials, 2020, 30, 1909919.	14.9	123
9	Zinc tin oxide as high-temperature stable recombination layer for mesoscopic perovskite/silicon monolithic tandem solar cells. Applied Physics Letters, 2016, 109, .	3.3	105
10	PERC+: industrial PERC solar cells with rear Al grid enabling bifaciality and reduced Al paste consumption. Progress in Photovoltaics: Research and Applications, 2016, 24, 1487-1498.	8.1	99
11	Notation= TeX >\$inbox{-}V\$⁢/tex>⁢/formula> Characteristics of ⁢formula formulatype="inline"> <tex notation="TeX">\$hbox{p}\$</tex> Polycrystalline Si/ <formula formulatype="inline"><tex Notation="TeX"&gt;\$hbox{n}\$</tex </formula> Monocrystalline Si, and <formula< td=""><td>2.5</td><td>91</td></formula<>	2.5	91
12	Junction Resistivity of Carrier-Selective Polysilicon on Oxide Junctions and Its Impact on Solar Cell Performance. IEEE Journal of Photovoltaics, 2017, 7, 11-18.	2.5	91
13	Parasitic Absorption in Polycrystalline Si-layers for Carrier-selective Front Junctions. Energy Procedia, 2016, 92, 199-204.	1.8	77
14	26.1%â€efficient POLOâ€IBC cells: Quantification of electrical and optical loss mechanisms. Progress in Photovoltaics: Research and Applications, 2019, 27, 950-958.	8.1	76
15	Interdigitated back contact solar cells with polycrystalline silicon on oxide passivating contacts for both polarities. Japanese Journal of Applied Physics, 2017, 56, 08MB15.	1.5	75
16	Maximizing tandem solar cell power extraction using a three-terminal design. Sustainable Energy and Fuels, 2018, 2, 1141-1147.	4.9	67
17	Separating the two polarities of the POLO contacts of an 26.1%-efficient IBC solar cell. Scientific Reports, 2020, 10, 658.	3.3	66
18	Improvement of the SRH bulk lifetime upon formation of n-type POLO junctions for 25% efficient Si solar cells. Solar Energy Materials and Solar Cells, 2017, 173, 85-91.	6.2	65

#	Article	IF	CITATIONS
19	Pinhole density and contact resistivity of carrier selective junctions with polycrystalline silicon on oxide. Applied Physics Letters, 2017, 110, .	3.3	61
20	A simple method for pinhole detection in carrier selective POLO-junctions for high efficiency silicon solar cells. Solar Energy Materials and Solar Cells, 2017, 173, 106-110.	6.2	56
21	Temperature-dependent contact resistance of carrier selective Poly-Si on oxide junctions. Solar Energy Materials and Solar Cells, 2018, 185, 425-430.	6.2	54
22	A Taxonomy for Three-Terminal Tandem Solar Cells. ACS Energy Letters, 2020, 5, 1233-1242.	17.4	51
23	Perimeter Recombination in 25%-Efficient IBC Solar Cells With Passivating POLO Contacts for Both Polarities. IEEE Journal of Photovoltaics, 2018, 8, 23-29.	2.5	49
24	On the recombination behavior of p <sup><i>+</i></sup> -type polysilicon on oxide junctions deposited by different methods on textured and planar surfaces. Physica Status Solidi (A) Applications and Materials Science, 2017, 214, 1700058.	1.8	48
25	Three-terminal III–V/Si tandem solar cells enabled by a transparent conductive adhesive. Sustainable Energy and Fuels, 2020, 4, 549-558.	4.9	46
26	Recombination Behavior of Photolithography-free Back Junction Back Contact Solar Cells with Carrier-selective Polysilicon on Oxide Junctions for Both Polarities. Energy Procedia, 2016, 92, 412-418.	1.8	42
27	Breakdown of the efficiency gap to 29% based on experimental input data and modeling. Progress in Photovoltaics: Research and Applications, 2016, 24, 1475-1486.	8.1	41
28	Evolutionary PERC+ solar cell efficiency projection towards 24% evaluating shadow-mask-deposited poly-Si fingers below the Ag front contact as next improvement step. Solar Energy Materials and Solar Cells, 2020, 212, 110586.	6.2	36
29	Ion diffusion and mechanical losses in mixed alkali glasses. Journal of Non-Crystalline Solids, 2006, 352, 5178-5187.	3.1	31
30	Equivalent Performance in Three-Terminal and Four-Terminal Tandem Solar Cells. IEEE Journal of Photovoltaics, 2018, 8, 1584-1589.	2.5	31
31	Backâ€contacted bottom cells with three terminals: Maximizing power extraction from currentâ€mismatched tandem cells. Progress in Photovoltaics: Research and Applications, 2019, 27, 410-423.	8.1	31
32	Present status and future perspectives of bifacial PERC+ solar cells and modules. Japanese Journal of Applied Physics, 2018, 57, 08RA01.	1.5	29
33	From PERC to Tandem: POLO- and p <sup>+</sup> /n <sup>+</sup> Poly-Si Tunneling Junction as Interface Between Bottom and Top Cell. IEEE Journal of Photovoltaics, 2019, 9, 49-54.	2.5	29
34	For none, one, or two polarities—How do POLO junctions fit best into industrial Si solar cells?. Progress in Photovoltaics: Research and Applications, 2020, 28, 503-516.	8.1	28
35	Simulation-based roadmap for the integration of poly-silicon on oxide contacts into screen-printed crystalline silicon solar cells. Scientific Reports, 2021, 11, 996.	3.3	24
36	Driving mechanisms for the formation of nanocrystals by annealing of ultrathin Ge layers in <mml:math <="" td="" xmlns:mml="http://www.w3.org/1998/Math/MathML"><td>3.9 .</td><td>21</td></mml:math>	3.9 .	21

36 display="inline"><mml:mrow><mml:msub><mml:mrow><mml:mtext>SiO</mml:mtext></mml:mrow><mml:mn>2

#	Article	IF	CITATIONS
37	Ultraâ€Thin Polyâ€&i Layers: Passivation Quality, Utilization of Charge Carriers Generated in the Polyâ€&i and Application on Screenâ€Printed Doubleâ€&ide Contacted Polycrystalline Si on Oxide Cells. Solar Rrl, 2020, 4, 2000177.	5.8	21
38	Internal Friction and Vulnerability of Mixed Alkali Glasses. Physical Review Letters, 2005, 95, 115901.	7.8	20
39	Modeling recombination and contact resistance of poly‣i junctions. Progress in Photovoltaics: Research and Applications, 2020, 28, 1289-1307.	8.1	20
40	Structural Investigation of Printed Ag/Al Contacts on Silicon and Numerical Modeling of Their Contact Recombination. IEEE Journal of Photovoltaics, 2016, 6, 1175-1182.	2.5	19
41	Building Blocks for Industrial, Screen-Printed Double-Side Contacted POLO Cells With Highly Transparent ZnO:Al Layers. IEEE Journal of Photovoltaics, 2018, , 1-7.	2.5	19
42	High Temperature Annealing of ZnO:Al on Passivating POLO Junctions: Impact on Transparency, Conductivity, Junction Passivation, and Interface Stability. IEEE Journal of Photovoltaics, 2019, 9, 89-96.	2.5	19
43	Changes in hydrogen concentration and defect state density at the poly-Si/SiOx/c-Si interface due to firing. Solar Energy Materials and Solar Cells, 2021, 231, 111297.	6.2	19
44	Evolution of oxide disruptions: The (W)hole story about poly-Si/c-Si passivating contacts. , 2016, , .		18
45	Determination of the <mml:math <br="" xmlns:mml="http://www.w3.org/1998/Math/MathML">display="inline"&gt;<mml:mrow><mml:mtext>Ge-nanocrystal</mml:mtext><mml:mo>/</mml:mo><mml:msub><mr interface trap density from the small signal response of charge stored in the nanocrystals. Physical Review B. 2010. 82</mr </mml:msub></mml:mrow></mml:math>	nl;mrow>	۲ איז
46	Toward Low-Cost 4-Terminal GaAs//Si Tandem Solar Cells. ACS Applied Energy Materials, 2019, 2, 2375-2380.	5.1	17
47	Degradation and Regeneration of <i>n</i> <sup>+</sup> -Doped Poly-Si Surface Passivation on <i>p</i> -Type and <i>n</i> -Type Cz-Si Under Illumination and Dark Annealing. IEEE Journal of Photovoltaics, 2020, 10, 423-430.	2.5	17
48	Monolithic Perovskite/Silicon Tandem Solar Cells Fabricated Using Industrial pâ€Type Polycrystalline Silicon on Oxide/Passivated Emitter and Rear Cell Silicon Bottom Cell Technology. Solar Rrl, 2022, 6, .	5.8	17
49	26%-efficient and 2 cm narrow interdigitated back contact silicon solar cells with passivated slits on two edges. Solar Energy Materials and Solar Cells, 2019, 200, 110021.	6.2	16
50	Introducing pinhole magnification by selective etching: application to poly-Si on ultra-thin silicon oxide films. Energy Procedia, 2017, 124, 435-440.	1.8	14
51	716 mV Openâ€Circuit Voltage with Fully Screenâ€Printed <i>p</i> â€Type Back Junction Solar Cells Featurir an Aluminum Front Grid and a Passivating Polysilicon on Oxide Contact at the Rear Side. Solar Rrl, 2021, 5, .	ig 5.8	14
52	A 22.3% Efficient pâ€Type Back Junction Solar Cell with an Alâ€Printed Frontâ€Side Grid and a Passivating n <sup>+</sup> â€Type Polysilicon on Oxide Contact at the Rear Side. Solar Rrl, 2020, 4, 2000435.	5.8	13
53	Optimization of four terminal rear heterojunction GaAs on Si interdigitated back contact tandem solar cells. Applied Physics Letters, 2021, 118, .	3.3	13
54	Optimized Metallization for Interdigitated Back Contact Silicon Heterojunction Solar Cells. Solar Rrl, 2017, 1, 1700021.	5.8	12

#	Article	IF	CITATIONS
55	Firing stability of tube furnaceâ€annealed nâ€type polyâ€Si on oxide junctions. Progress in Photovoltaics: Research and Applications, 2022, 30, 49-64.	8.1	12
56	UV radiation hardness of photovoltaic modules featuring crystalline Si solar cells with AlO <i><sub>x</sub></i> /p <sup>+</sup> â€type Si and SiN <i><sub>y</sub></i> /n <sup>+</sup> â€type Si interfaces. Physica Status Solidi - Rapid Research Letters, 2017, 11, 1700178.	2.4	11
57	Photonic crystals for highly efficient silicon single junction solar cells. Solar Energy Materials and Solar Cells, 2021, 233, 111337.	6.2	11
58	Local Enhancement of Dopant Diffusion from Polycrystalline Silicon Passivating Contacts. ACS Applied Materials & Interfaces, 2022, 14, 17975-17986.	8.0	11
59	High time resolution measurement of solar irradiance onto driving car body for vehicle integrated photovoltaics. Progress in Photovoltaics: Research and Applications, 2022, 30, 543-551.	8.1	11
60	Basic Study on the Influence of Glass Composition and Aluminum Content on the Ag/Al Paste Contact Formation to Boron Emitters. Energy Procedia, 2015, 67, 20-30.	1.8	10
61	Fully screenâ€printed silicon solar cells with local Alâ€p <sup>+</sup> and nâ€type POLO interdigitated back contacts with a <i>V</i> <sub>OC</sub> of 716 mV and an efficiency of 23%. Progress in Photovoltaics: Research and Applications, 2021, 29, 516-523.	8.1	10
62	Towards 28 %-efficient Si single-junction solar cells with better passivating POLO junctions and photonic crystals. Solar Energy Materials and Solar Cells, 2022, 238, 111560.	6.2	10
63	On the chances and challenges of combining electronâ€collecting <i>n</i> POLO and holeâ€collecting Alâ€ <i>p</i> <sup>+</sup> contacts in highly efficient <i>p</i> â€type câ€Si solar cells. Progress in Photovoltaics: Research and Applications, 2023, 31, 327-340.	8.1	9
64	PE-CVD fabrication of germanium nanoclusters for memory applications. Materials Science and Engineering B: Solid-State Materials for Advanced Technology, 2008, 147, 213-217.	3.5	8
65	Electrical characterization and modelling of <i>n–n</i> Ge-Si heterojunctions with relatively low interface state densities. Journal of Applied Physics, 2012, 112, .	2.5	8
66	Increased Front Surface Recombination by Rear-Side Laser Processing on Thin Silicon Solar Cells. IEEE Journal of Photovoltaics, 2013, 3, 976-984.	2.5	8
67	Transferring the Record p-type Si POLO-IBC Cell Technology Towards an Industrial Level. , 2019, , .		8
68	Nanostructured front electrodes for perovskite/c-Si tandem photovoltaics. Optics Express, 2020, 28, 8878.	3.4	8
69	ZnO:Al/a-SiOx front contact for polycrystalline-silicon-on-oxide (POLO) solar cells. AIP Conference Proceedings, 2018, , .	0.4	7
70	Demonstration of Feeding Vehicleâ€Integrated Photovoltaicâ€Converted Energy into the Highâ€Voltage Onâ€Board Network of Practical Light Commercial Vehicles for Range Extension. Solar Rrl, 2022, 6, 2100516.	5.8	7
71	Single-Electron Charging and Discharging Analyses in Ge-Nanocrystal Memories. IEEE Transactions on Electron Devices, 2011, 58, 376-383.	3.0	6
72	Dopant diffusion from p <sup>+</sup> -poly-Si into c-Si during thermal annealing. , 2016, , .		6

#	Article	IF	CITATIONS
73	Increasing the photo-generated current in solar cells with passivating contacts by reducing the poly-Si deposition temperature. AIP Conference Proceedings, 2018, , .	0.4	6
74	Three-Terminal Bipolar Junction Bottom Cell as Simple as PERC: Towards Lean Tandem Cell Processing. , 2019, , .		6
75	Two-level Metallization and Module Integration of Point-contacted Solar Cells. Energy Procedia, 2014, 55, 361-368.	1.8	5
76	Contacting a single nanometerâ€sized pinhole in the interfacial oxide of a polyâ€silicon on oxide (POLO) solar cell junction. Progress in Photovoltaics: Research and Applications, 2021, 29, 936-942.	8.1	5
77	Role of oxygen in the UV-ps laser triggered amorphization of poly-Si for Si solar cells with local passivated contacts. Journal of Applied Physics, 2021, 129, .	2.5	5
78	Light and elevated temperature induced degradation and recovery of gallium-doped Czochralski-silicon solar cells. Scientific Reports, 2022, 12, 8089.	3.3	5
79	PECVD grown Ge nanocrystals embedded in : From disordered to templated self-organization. Microelectronics Journal, 2009, 40, 759-761.	2.0	4
80	ITO-free metallization for interdigitated back contact silicon heterojunction solar cells. Energy Procedia, 2017, 124, 379-383.	1.8	4
81	Notice of Removal Junction resistivity of carrier selective polysilicon on oxide junctions and its impact on the solar cell performance. , 2017, , .		4
82	Still in the game. Nature Energy, 2021, 6, 333-334.	39.5	4
83	Evaluation of localized vertical current formation in carrier selective passivation layers of silicon solar cells by conductive AFM. AIP Conference Proceedings, 2019, , .	0.4	3
84	Interface defect-assisted single electron charging (and discharging) dynamics in Ge nanocrystals memories. Applied Physics Letters, 2010, 97, .	3.3	2
85	Silicon nanopowder as diffuse rear reflector for silicon solar cells. Journal of Applied Physics, 2017, 122, .	2.5	2
86	Specifications for maximum power point tracking in vehicle-integrated photovoltaics based on high-resolution transient irradiance measurements. , 2020, , .		2
87	Rear side dielectrics on interdigitating p+-(i)-n+ back-contact solar cells â^' hydrogenation vs. charge effects. EPJ Photovoltaics, 2021, 12, 6.	1.6	2
88	Hierarchical Etching for Improved Optical Front-side Properties of Monocrystalline Si Solar Cells. Energy Procedia, 2015, 77, 810-815.	1.8	1
89	Inkjet-Printed <i>In Situ</i> Structured and Doped Polysilicon on Oxide Junctions. IEEE Journal of Photovoltaics, 2021, 11, 1149-1157.	2.5	1
90	Simulation of solar cell performance based on in the field measured ambience parameters. AIP Conference Proceedings, 2019, , .	0.4	0

#	Article	IF	CITATIONS
91	2D Surface Passivation in Semi-transparent Perovskite Top Solar Cells with Engineered Bandgap for Tandem Photovoltaics. , 2020, , .		0
92	Perovskite Tandem Photovoltaics: Employing 2D/3D Perovskite Heterostructure for Perovskite Top Solar Cell with Engineered Bandgap. , 0, , .		0
93	A round Robin-Highliting on the passivating contact technology. EPJ Photovoltaics, 2021, 12, 12.	1.6	0